Electrophoretic Deposition of CdSe Nanocrystal Films on Conducting Electrodes

Mohammad A. Islam[a], Yuqi Xia[b], Benjamin J. Kraines, and Irving P. Herman[a]
[a]Department of Applied Physics and Applied Mathematics
[b]Department of Physics
Materials Research Science and Engineering Center
Columbia University, New York, NY 10027, U.S.A.

ABSTRACT

A dc electric field is used to attract thermally charged CdSe nanocrystals in solution to rapidly form large-area, micron-thick films of equal thickness on both electrodes. A pair of Au-on-Si or conducting ITO-on-glass electrodes was submerged in the nanoparticle solution and a dc voltage was applied in a dark room. Uniform, robust, very smooth, and apparently identical films formed on both electrodes. Photoluminescence and absorption of the films showed that they are indeed made of dense arrays of individual nanocrystals. The deposition implies there are both positively and negatively thermally charged dots in solution. These high quality dense arrays of the nanoparticles could be useful in several applications.

INTRODUCTION

The formation of arrays and films of nanoparticles is important for exploring properties of high densities of these dots and for applications. Semiconductor [1], metal [2] and magnetic nanocrystals [3] have been self-assembled to make quantum dot superlattices. Superlattices made from nanoparticles enable the study of the evolution of collective effects from individual dot properties. Semiconductor nanoparticles are important for their optical properties, which can be used, for example, in light emitting diodes (LEDs) [4] and in biological labeling [5].

Choosing a surface for the nanocrystal film deposition is an important consideration. For example, for electronic devices it might be necessary to deposit on unpatterned or patterned electrodes, such as Au-on-Si surfaces; whereas for LEDs it may be necessary for the surface to be conducting and transparent, such as ITO-on-glass. Currently, films of nanoparticles are formed mostly by dry casting or spin coating. These films are not very uniform. Both methods depend on the particle-particle and particle-substrate interactions as a drop of the nanoparticle solution is left to dry on a substrate. However, most suitable solvents are extremely volatile and rapid dewetting of these solvents significantly undermines the long range ordering and film quality. Consequently, most of the nanocrystal superlattices formed using these methods have domain sizes less than a few hundred nanometers [6-9]. Also, such dry cast and spun on films are unpatterned. For many applications, films of controlled thickness over controlled regions may be needed.

We report here on the electrophoretic deposition of CdSe nanocrystals with diameter in the range of 2.8 nm to 4.1 nm on Au-on-Si electrodes and on ITO-on-glass electrodes to form very high quality films. This continues the work first reported by the authors in Ref. [10]. The nanocrystals were found to deposit on both the anode and the cathode, unlike in conventional electrophoretic deposition, and resulted in excellent quality films of controlled thickness. The nanoparticle films were very smooth. These films do not dissolve in hexane (as do those formed by dry casting), which is a good solvent for these nanoparticles.

EXPERIMENTAL PROCEDURE

CdSe nanocrystals of diameter in the range of 2.8 nm to 4.1 nm capped by tri n-octylphosphineoxide (TOPO) were synthesized according to the method of Murray *et al.* [11]. Solutions of these nanoparticles were made with hexane solvent, with densities between 1×10^{14} and 1×10^{16} dots/cc. Au-on-Si electrodes were prepared by depositing ~10 nm Ti and then ~150 nm Au on 0.8 × 1.4 cm rectangular sections of Si(100) wafers. ITO-on-aluminosilicate glass electrodes (100 nm thick ITO) with sheet resistance of $10 \pm 5\ \Omega$ were purchased from Delta Technologies. Prior to the experiments, the ITO electrodes were cleaned by ultrasonicating first with detergents and then with a 50/50 mixture of acetone and iso-propanol, and then rinsed with hot de-ionized water. A pair of electrodes (usually Au-Au or ITO-ITO) was separated by ~2.0 mm and were submerged in a beaker with the nanoparticle solution. DC voltages up to 1000 V were applied across the electrodes at room temperature in the dark, with solvent added as needed to counter any solvent evaporation. DC current was monitored during runs, and the deposits on the electrodes were examined afterwards using visible microscopy, atomic force microscopy (AFM), scanning electron microscopy (SEM), and profilometry. The absorption spectrum of the nanoparticle solution was measured using a UV-VIS spectrophotometer to determine the density of the nanoparticles in the solution before and after deposition. Absorption and photoluminescence (PL) spectra of the films were obtained during processing. In some experiments the Au electrodes were prepatterned using standard optical lithography methods.

RESULTS AND DISCUSSION

Deposition of CdSe nanocrystals on Au electrodes

For the electrophoretic deposition of 3.2 nm diameter CdSe dots on unpatterned Au-on-Si electrodes, the initial current density between the electrodes was ~20.8 nA/cm^2 for 530 V applied (2.5×10^5 V/m) and 2.6×10^{14} dots/cc; the current density was linearly proportional to both voltage V and particle density n; it decreased to ~9.5 nA/cm^2 in 30 minutes as shown in Fig. 1. Without the dots, the current was ~100× smaller with the hexane solvent only and 20× smaller with TOPO dissolved in hexane (with TOPO mass half that of the usual dot mass).

After long runs (30 min, 530 V, 2.6×10^{14} dots/cc), 0.76 μm-thick, apparently identical films were deposited on both electrodes, as shown in the visible micrograph in Fig. 2. Strain in the film relaxes when the film thickness exceeds 0.8 μm and there is cracking, as is seen in the SEM image of a 1.2 μm thick film in the inset of Fig. 2. Cracking due to solvent evaporation is a common phenomenon during film drying [12]. Such strain and strain relaxation in these films will be discussed further in a subsequent publication.

The initial deposition rate was ~ (7.97×10^{-4} nm/s) V(in volts) n(in 2.6×10^{14} dots/cc), per electrode. No deposit was formed without the voltage. Visible microscopy, AFM, SEM, and profilometry showed that films on both electrodes were very smooth, with ~10-20 nm roughness.

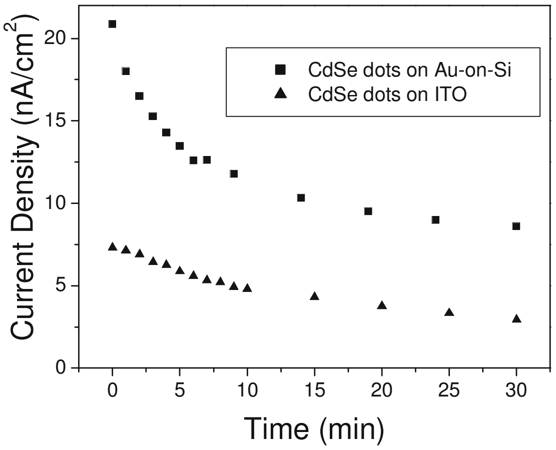

Figure 1. Current vs. time during the electrophoretic deposition of CdSe nanocrystals on Au-on-Si and ITO-on-glass electrodes.

Figure 2. Large area (~0.25 cm) optical microscope image of the 0.76 μm-thick electrodeposited CdSe nanocrystal film on a Au electrode. Also shown is the SEM image of a 1.2 μm thick, cracked film in the inset. The films on the negative electrodes were the same as those shown here on the positive electrode.

Photoluminescence spectra of these films showed one sharp peak near 567 nm (exciton emission) as shown in Fig. 3, and a broader and much weaker feature to the red of the 567 nm peak. The film PL was found to be stable for at least 6 months. In dot solution there is a 541 nm absorption and 560 nm PL peak. The strong 567 nm PL peak of the film shows that the films consist of CdSe nanocrystals that are not greatly changed from solution (same radius, most or all the caps remain intact etc). The 27 meV red shift of the electrodeposited films PL from that of

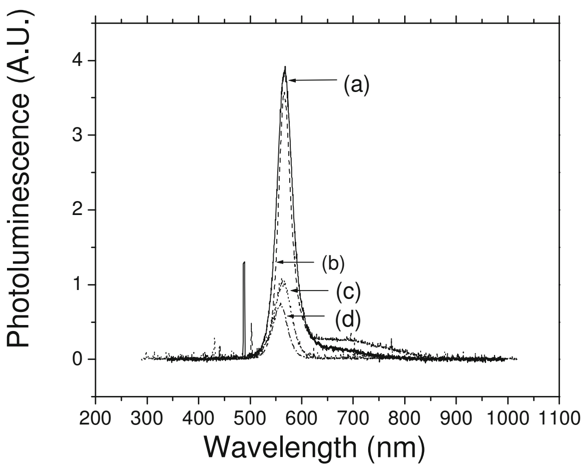

Figure 3. PL of the (a) 0.76 μm thick electrodeposited CdSe film on Au electrode, (b) 0.52 μm thick electrodeposited CdSe film on ITO electrode, (c) dry cast film, and (d) dot solution.

the solution is due to fast interdot radiative transfer between nearby dots to larger, lower-band-gap dots [13]; this is also seen in the weaker PL from dry cast films.

The films were robust. After drying, these films did not dissolve in hexane (as do those formed by dry casting and spin coating), even when voltage of either polarity was applied across it to a bare Au electrode.

The loss of dots in the solution due to deposition was tracked using absorption, calibrated by the mass of the dry dots (with TOPO capping) and compared to the number of dots deposited. The number of dots lost from the nanoparticle solution due to deposition was estimated by

$$N_{\mathrm{lost}} = (A_{\mathrm{before}} - A_{\mathrm{after}}) \times \text{calibration factor} \tag{1}$$

where A_{before} is the absorbance at the 541 nm first exciton peak of the nanoparticle solution before deposition and A_{after} is that after deposition, as shown in Fig. 4.

The number of dots deposited was approximated as

$$N_{\mathrm{dep}} = 0.74At/(4\pi R^3/3), \tag{2}$$

where A is the total electrode area, t is the film thickness (same for each electrode), R is the effective radius of each dot including capping ligand (2.15 nm for 3.2 nm diameter dots with an ~1.1 nm long TOPO cap [14]) and the 0.74 assumes fcc packing. N_{dep} was typically less than N_{lost} by ~28%. This difference is attributable to systematic errors in the determination of absorption cross-section and particle diameter, less than close-packing densities, and film cracking.

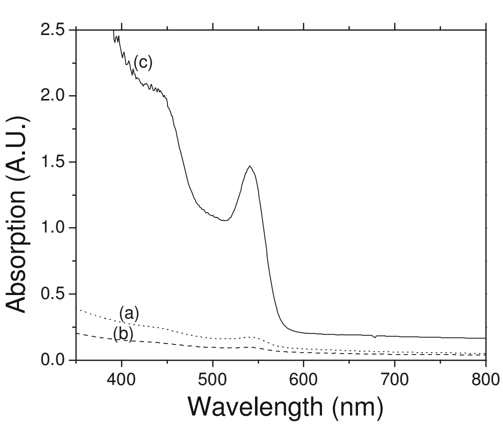

Figure 4. Absorption spectrum of nanocrystal solution (a) before and (b) after electrodeposition, and of (c) electrodeposited CdSe nanoparticle film on the positive ITO electrode.

The total number of elementary charges collected was calculated by integrating the current vs. time plot of Fig. 1 and was compared to the number of nanoparticles deposited. It was found that for the 3.2 nm diameter CdSe nanoparticles, ~33 nanocrystals were deposited for each elementary charge collected. This is discussed later.

Deposition of CdSe nanocrystals on ITO electrodes

During electrophoretic deposition of 3.2 nm diameter CdSe dots on ITO-on-glass electrodes, the initial current density between the electrodes was ~7.3 nA/cm^2 for 530 V (2.7 $\times 10^5$ V/m) and 2.65×10^{14} dots/cc. The current density was linearly proportional to both V and n and decreased to ~ 2.9 nA/cm^2 in 30 minutes, as shown in Fig. 1.

As with the Au electrodes, uniform, apparently identical films formed on both ITO electrodes. After long runs (30 min, 530 V, 2.65×10^{14} dots/cc), 0.52 μm-thick films were deposited on both electrodes, as shown in Fig. 5. No deposit was formed without the voltage. These films on ITO were also robust and also crack when the film thickness exceeds 0.8 μm.

PL of these films was similar to those on the Au electrodes as shown in Fig. 3. Unlike the films grown on Au-on-Si electrodes, the substrate was transparent and permitted the collection of absorption spectrum, by transmission, as shown in Fig. 4. The absorption spectrum of the film is much sharper than that of the solution and has the same peak location as that of the solution.

Deposition of patterned films

Figure 6 shows deposition on electrodes with Au/Ti films patterned on 0.2 μm-thick silicon dioxide. Deposition, occurs selectively only on top of the Au connected to the electrode

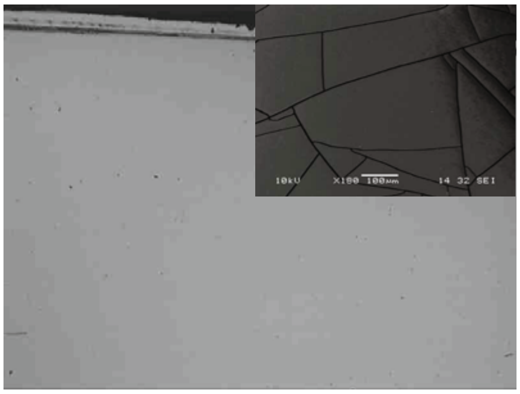

Figure 5. Large area (~0.25 cm) optical microscope image of the (uncracked) 0.52 µm thick electrodeposited CdSe dot film on the ITO electrode. Also shown is the SEM image of a 2.4 µm thick cracked film in the inset. The films on the negative electrodes were the same as those shown here on the positive electrode.

shown in the SEMs (regions A); there was very little or no deposition on the bare oxide (B) and patterned gold regions not electrically connected to the electrode (C), as confirmed by profilometry traces in this figure. Patterned CdSe dot films as narrow as 1 µm have been demonstrated [10].

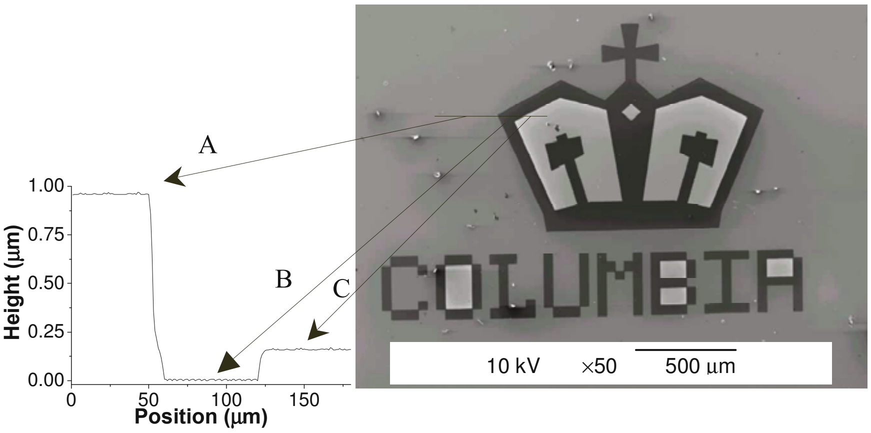

Figure 6. Selective electrodeposition of 0.8 µm thick films of CdSe nanocrystals on top of patterned Au films - connected to the electrode - atop 0.2 µm thick silicon dioxide (regions A), with very little or no deposition on the bare oxide (B) and patterned gold regions not electrically connected to the electrode (C). The profilometry scan for the SEM shows the thickness for regions (A) [0.8 µm thick dot film atop 0.15 µm thick Au film], (B), and (C) [unconnected 0.15 µm thick Au film].

Deposition mechanism

Most electrophoretic studies of depositing layers of charged particles on electrodes have been conducted in aqueous solutions, such as water, in which the solvent played a major role in conduction of current, the effective particle charge and charge screening. The applied voltages were much lower in those cases, often in the vicinity of ~1 V and deposition was on only one electrode [15,16]. The hexane solvent used here carries very small, if not zero, current, is very "inert" in polarizing the dissolved medium, and screening. Also, deposition takes place on both electrodes. Elements of the deposition mechanism here are clear, but parts are still unclear.

Most of the current is thought to be from positively and negatively charged nanocrystals, which have equal densities. The importance of counter ions seems small, though the role of these ions cannot be totally discounted. The sticking of nanocrystals to the electrodes to form films is much more sensitive to the conditions of the solution (impurities, etc.) than to the flow of current. Under some conditions it could be less than unity, but as seen above, under usual conditions many more dots than charges are collected. In these experiments the decrease in current flow seems to follow the loss of nanocrystals in solution. The charge of virtually every nanocrystal impinging on an electrode is neutralized. This charge is presumed to be balanced by a charge flowing in the external circuit. It is also possible, but less likely that the charged dots remain charged on the electrode and are balanced by charges from the external circuit forming a dipole layer or that the charged dots reaching an electrode are neutralized by counter ions in the solution.

As seen from Fig. 1, the current density with the ITO-on-glass electrodes is about a third of that with Au-on-Si electrodes. This could be due to the larger resistivity of the ITO electrode ($8 \times 10^{-6}\ \Omega$-m) than the Au electrode ($8 \times 10^{-8}\ \Omega$-m), and consequently the larger ITO film resistance. The deposition rate with the ITO electrodes is about two-thirds that with Au.

Thermal charging of CdSe, ZnSe and Au nanoparticles in solution has been discussed by Shim *et al.* [17]. Similar observations have been made here. The initial dc conductivity of the 3.2 nm CdSe/hexane solution was $\sigma = 7.86 \times 10^{-10}\ \Omega^{-1}\ \mathrm{m}^{-1}$. The conductivity of a solution of charged spheres of density n_{charged} in a solvent of viscosity η can be calculated using the Einstein-Nernst equation

$$\sigma = n_{\mathrm{charged}} e^2 / 6\pi\eta R, \qquad (3)$$

where R is the hydrodynamic radius and e is the charge of each sphere.

If there are positive and negative dots with densities n_+ and n_-, then $n_{\mathrm{charged}} = n_+ + n_-$. If there are no other counter ions, then the equal film thickness on both electrodes suggests $n_+ = n_- = n_{\mathrm{charged}}/2$. Taking e as the elementary charge, $n_{\mathrm{charged}} = 3.90 \times 10^{11}$/cc, or 0.15% of the nanocrystals are charged, half positively and half negatively. If a larger charge per dot were assumed, n_{charged} would be smaller and the ratio of the number of deposited dots per charged dot would be larger. If much of the voltage drop were near the electrodes [18], the conductivity in the bulk solution would be much larger than calculated here. This would make n_+ and n_- larger, but not change the ratio of collected dots to charges.

More charges are collected than are initially in the beaker, which suggests fast diffusion of dots from outside the volume spanned by the electrodes in the beaker to this volume, and fast thermalization of the charging of dots.

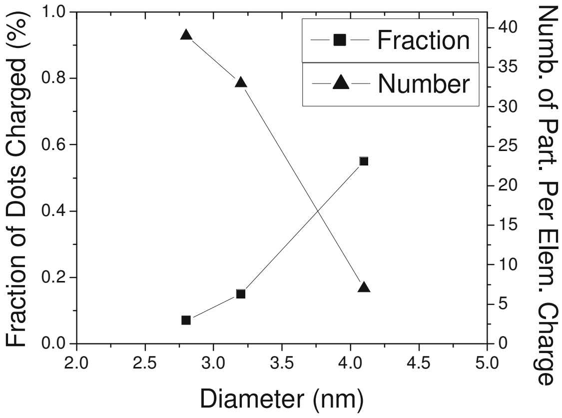

Figure 7. The percentage of charged nanocrystals and number of nanocrystals deposited for each elementary charge collected as a function of dot radius, for electrophoretic deposition on Au-on-Si electrodes.

The energy needed to put a charge on the core of these 3.2 nm dots can be estimated from $E = e^2/2R(1/\varepsilon_{\text{hexane}} - 1/\varepsilon_{\text{CdSe}})$. Using $\varepsilon_{\text{CdSe}} = 7.74$ and $\varepsilon_{\text{hexane}} = 1.96$ and $R = 1.6$ nm, this energy was found to be 0.17 eV. The fraction of charged dots scales as $\exp(-E/kT)$. (The fraction of charged nanoparticles in thermal equilibrium at room temperature is 0.15%, which happens to be close to the value of this Boltzmann factor ~0.13%.)

For 2.8 and 4.1 nm diameter nanoparticles, the fraction of the particles charged was found to be 0.07% and 0.55% respectively. The number of particles deposited for each elementary charge collected was 39 for 2.8 nm and 7 for 4.1 nm diameter particles. As shown in Fig. 7, the fraction of the charged nanoparticles increases as a function of nanoparticle radius, which is expected because the charging energy decreases. Also, the ratio of deposited dots to collected charges decreases with radius.

Only a fraction of a percent of the CdSe dots are charged and the number of nanoparticles deposited is much larger than the number of elementary charges collected. This suggests that uncharged dots are collected on the electrodes along with the charged dots. One way this can occur is by the dragging of some uncharged nanoparticles by the charged nanoparticles, by interactions with the induced or permanent [17] dipole moments of the uncharged dots. (Higher-order quadrupole interactions may also be important.) These dipolar dots would accumulate around the charged nanoparticles if this interaction energy (including any dipole-dipole interactions) exceeds kT during transport to an electrode. If this mechanism were important, the effective radius used in Eq. 3 would have to be larger, which would affect the determination of n_{charged}. Near the electrodes these dipoles could be influenced by electric field gradients arising from the roughness of the conducting electrode surface. (This would occur even without this dragging.) The uncharged dots could also be carried along by the hydrodynamic flows or gradients caused by the transport of the charged dots. Movement of objects under the influence of the hydrodynamic flows or the "wake" caused by other objects happens when the motion of the latter is fast and the motion is turbulent. It has been showed experimentally that when a particle is in a turbulent flow, it can either carry other particles along with it or propel other particles in the opposite direction [19, 20]. This does not seem likely here. It is also possible that each dot in the film represents a charged dot transported to the surface and that the number of collected charges is smaller than this because of interactions with the solvent, but this is unlikely given the relative independence of current flow to impurities in the solution.

Film properties, including electrical conductivity

The mechanical, thermal, optical, infrared, and electrical properties of these films are being investigated and will be reported on here and elsewhere. Electrical conductivity of the electrodeposited film on Au-on-Si substrate was measured for several reasons, illustrated in Fig. 8. The nature of charge transport in the dried films is of fundamental and practical interest. In published studies, the resistivity of spun-on [21] or dry cast [22] CdSe nanocrystal films was shown to depend on time, voltage and temperature. The electrophoretic films are more robust, which could suggest closer and/or more strongly bound dots, and this could affect charge transfer between the dots.

Charge transport across the electrophoretically growing film must occur for film growth to continue. Since the collected current tracks the density of dots remaining in solution, transport in the film does not seem to be a limiting factor. Measuring the resistivity of the dried film (Fig. 8(b)), can be followed by that of films in hexane *ex situ* (Fig. 8(c)). This *ex situ* measurement would simulate *in situ* deposition (Fig. 8(a)).

In preliminary measurements, at room temperature the resistance of an ~ 0.7 μm thick (uncracked) film was ~ 10 Ω (applied voltage 1 V, 1 mm x 1mm contact region – silver paste contacts, in the dark), with the main conductivity path being "down" through the CdSe dot film at the contacts, then across the gold film and then "up" through the CdSe dot film at the other contact. The resistivity can then be calculated from the measured resistance R

$$R = 2\rho_f(t_f/ a_c) + \rho_{Au}[d/(t_f\, a_c^{1/2})] \qquad (4)$$

Here ρ_f and ρ_{Au} are the electrical resistivities of the dot film and the Au substrate, respectively, t_f and t_{Au} are the thickness of the dot film and the Au film, respectively, a_c is the contact area and d is the distance between the contacts. With $a_c = 1$ mm^2 and $t_f = 0.7$ μm, the resistivity of the dot film was found to be ~7 Ω-m under these conditions, if we ignore the resistivity of Au. This is a preliminary measurement, and could be affected by time, voltage, temperature and the nature of the contacts. The formation of contacts to these films is still under investigation. Shadow-mask deposited Au films were sometimes shorted, suggesting the presence of some pinholes in the films.

If one assumes that ~7 Ω-m is also the resistivity of the wet film *in situ* during electrophoretic deposition (and this needs to be substantiated), the resistance across the whole film (~1 cm^2 area) during deposition would be ~0.05 Ω for each electrode. Since the typical resistance in the experiments is in the 10^{10} Ω range, the voltage drop is entirely across the hexane/dot solution.

CONCLUDING REMARKS

This new deposition method should be applicable to many or all nanocrystals and

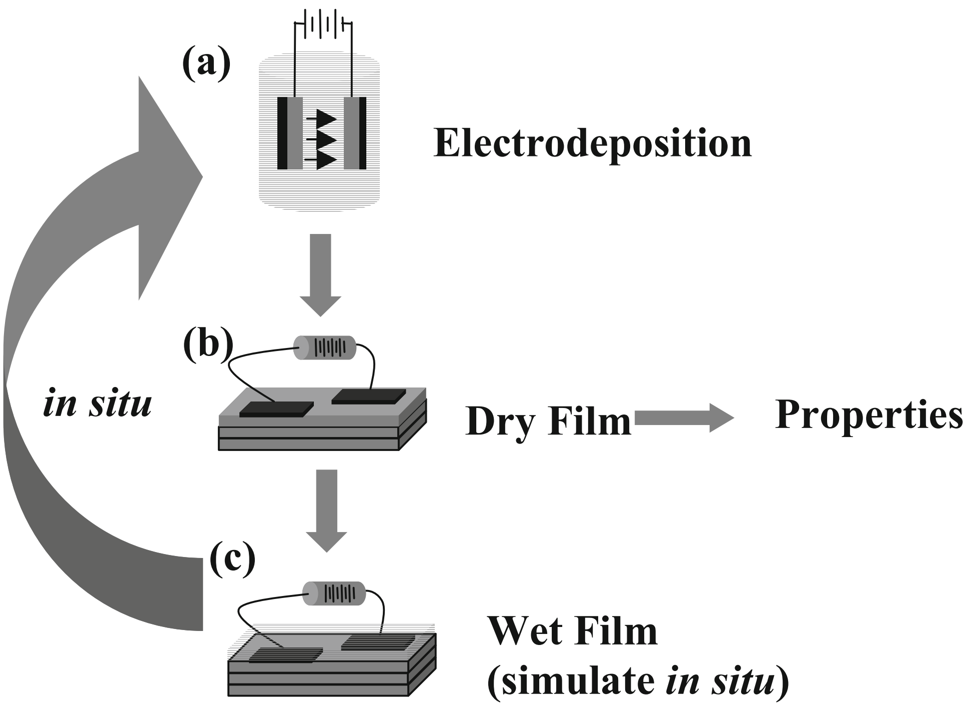

Figure 8. Simulation of *in situ* electrical conductivity measurement of the electrodeposited CdSe nanocrystal film. In (b) and (c) contacts are shown on the CdSe dot film atop a Au film atop the Si substrate.

nanorods, since thermal charging appears to be very common, and to mixtures of them. Simultaneous deposition of patterned films on both electrodes is feasible and the film thickness can be separately controlled for different electrodes on a substrate. One would expect ordered layers would form for slower deposition rates and very thin films. The electrophoretic deposition of films of other nanocrystals and of mixtures of different nanocrystals has been demonstrated by the authors and will be reported elsewhere.

ACKNOWLEDGMENTS

This work was primarily supported by the MRSEC program of the National Science Foundation, under Award Nos. DMR-9809687 and DMR-0213574. BJK was supported by the MRSEC REU program. The authors thank Tony F. Heinz for valuable conversations.

REFERENCES

1. C. B. Murray, C. R. Kagan, and M. G. Bawendi, *Science* **270**, 1335 (1995).
2. C. P. Collier, R. J. Saykally, J. J. Shiang, S. E. Henrichs, and J. R. Heath, *Science* **277**, 1978 (1997).
3. S. Sun, C. B. Murray, D. Weller, L. Folks, and A. Moser, *Science* **287**, 1989 (2000).
4. M. C. Schlamp, X. Peng, and A. P. Alivisatos, *J. Appl. Phys*. **82**, 5837 (1997).
5. X. Michalet, F. Pinaud, T. D. Lacoste, M. Dahan, M. P. Bruchez, A. P. Alivisatos, and S. Weiss, *Single Molecules* **2**, 261 (2001).
6. F. Remacle, C. P. Collier, G. Markovich, J. R. Heath, U. Banin, and R. D. Levine, *J. Phys. Chem.* **102**, 7727 (1998).
7. B. A. Korgel and D. Fitzmaurice, *Phys. Rev. Lett.* **80**, 3531 (1998).
8. P. C. Ohara and W. M. Gelbart, *Langmuir* **14**, 3418 (1998).
9. M. Gelbart, R. P. Sear, J. R. Heath, and S. Chaney, *Faraday Discuss.* **112**, 299 (1999).
10. M. A. Islam and I. P. Herman, *Appl. Phys. Lett*. **80**, 3823 (2002).
11. C. B. Murray, D. J. Norris, and M. G. Bawendi, *J. Am. Chem. Soc.* **115**, 8706 (1993).
12. A. Groisman and E. Kaplan, *Europhys. Lett.* **25**, 415 (1994).
13. C. R. Kagan, C. B. Murray, M. Nirmal, and M. G. Bawendi, *Phys. Rev. Lett*. **76**, 3403 (1996).
14. C. B. Murray, Ph. D. Thesis, Massachusetts Institute of Technology (1993).
15. M. Trau, D. A. Saville, and I. A. Aksay, *Science* **272**, 706 (1996).
16. M. Giersig and P. Mulvaney, *Langmuir* **9**, 3409 (1993).
17. M. Shim and P. Guyot-Sionnest, *J. Chem. Phys.* **111**, 6955 (1999).
18. P. Sarkar and P. S. Nicholson, *J. Am. Chem. Soc.* **79**, 1987 (1996).
19. M. Whittle, *J. Non-Newt. Fl. Mech.* **37**, 233 (1990).
20. S. Lee, *Computers and Fluids* **29**, 639 (2000).
21. D. S. Ginger and N. C. Greenham*, J. Appl. Phys*. **87**, 1361 (2002).
22. N. Y. Morgan, C. A. Leatherdale, M. Drndic, M. V. Jarosz, M. C. Kastner, and M. G. Bawendi, *Phys. Rev. B* **66**, 075339 (2002).